Macromolecules
ARTICLE

Macromolecules **2010**, *43*, 1227–1235 **1227**
DOI: 10.1021/ma902447p

Synthesis, Characterization, and Properties of Starlike Poly(*n*-butyl acrylate)-*b*-poly(methyl methacrylate) Block Copolymers

Alper Nese,[†] Jaroslav Mosnáček,[†,‡] Azhar Juhari,[§] Jeong Ae Yoon,[†] Kaloian Koynov,[§] Tomasz Kowalewski,[†] and Krzysztof Matyjaszewski*,[†]

[†]*Department of Chemistry, Carnegie Mellon University, 4400 Fifth Avenue, Pittsburgh, Pennsylvania 15213,* [‡]*Polymer Institute, Centre of Excellence GLYCOMED, Slovak Academy of Sciences, Dúbravská cesta 9, 842 36 Bratislava, Slovakia, and* [§]*Max Planck Institute for Polymer Research, Ackermannweg 10, 55128 Mainz, Germany*

Received November 5, 2009; Revised Manuscript Received December 24, 2009

ABSTRACT: A series of 10- and 20-arm starlike block copolymers containing inner soft poly(*n*-butyl acrylate) (PBA) block and outer hard poly(methyl methacrylate) (PMMA) block were synthesized by atom transfer radical polymerization (ATRP). Short macroinitiators for preparation of starlike copolymers, poly(2-bromoisobutyryloxyethyl acrylate) (PBiBEA) with degree of polymerization DP = 10 and 20, was prepared by ATRP of trimethylsilyloxyethyl acrylate (HEATMS) and subsequently esterified. Partial star coupling during the star extension with PMMA blocks was observed, and the coupling increased with increasing number of arms and arm length. Phase-separated morphologies of cylindrical hard PMMA block domains arranged in the soft PBA matrix were observed by atomic force microscopy and small-angle X-ray scattering. The mechanical and thermal properties of the copolymers were also thoroughly characterized, and their thermoplastic elastomer behavior was studied. Tensile strength of the starlike copolymers was considerably higher compared to linear and three-arm stars with similar compositions.

Introduction

In recent years, synthesis of polymers with brush,[1,2] star-shaped,[3,4] and hyperbranched[5,6] molecular architecture has attracted much interest due to their different properties from those of linear polymers. Expansion in the synthesis of such polymers was allowed due to broad evolution of various controlled polymerization techniques such as anionic polymerization,[7] ring-opening metathesis polymerization,[8] and controlled/living radical polymerizations,[9] including cobalt-mediated polymerization,[10] nitroxide-mediated polymerization,[11] reversible addition−fragmentation transfer,[12,13] or atom transfer radical polymerization (ATRP).[14−18] Recently, many efforts were made to prepare well-defined star polymers. For the synthesis of star-shaped polymers two major strategies, arm-first and core-first, can be employed. The arm-first technique involves use of multifunctional linking agent for binding of preformed polymer chains.[19−23] The core-first strategy utilizes multifunctional initiators from which polymer chains are grown.[24−32] For example, dipentaerythritol derivatives having four and six hydroxyl groups[28] and polyglycidol[29] were used as initiators for ring-opening polymerization of lactones. Moreover, cores having various numbers of hydroxyl groups were brominated and used for the ATRP of vinyl monomers.[24]

Recently, it was demonstrated that thermoplastic elastomers based on star block copolymers may exhibit improved properties in comparison with the linear ABA triblock copolymers.[33−39] For example, multiarm polystyrene-*b*-polyisobutylene (PS-*b*-PIB) star block copolymers have shown much lower sensitivity to diblock contamination and substantially better mechanical properties than their linear triblock counterparts.[35]

*Corresponding author. E-mail: km3b@andrew.cmu.edu.

Herein we report a new approach for the preparation of the starlike polymers by grafting polymer chains from very short linear multifunctional initiators. Similar, but much longer, macroinitiators have been used for synthesis of molecular brushes, with a much higher aspect ratio or a length of a backbone vs side chains.[2,40−44] Herein, the side chains are much longer than backbone, resulting in rather the starlike structures. The relative asymmetry of the stars should depend on the aspect ratio (Scheme 1). ATRP was used for both preparation of the multifunctional initiator and the consecutive arm growth. The arm extension of living arm ends was performed to form starlike block copolymers. We have studied the morphology and the mechanical properties of the prepared copolymers and compared their thermoplastic elastomer characteristics with those of the corresponding linear triblock ABA copolymers.

Experimental Section

Materials. 2-Hydroxyethyl acrylate (HEA) (96%) was purchased from Aldrich. *n*-Butyl acrylate (BA) and methyl methacrylate (MMA) were purchased from Acros. All monomers were purified by passing through a basic alumina column to remove the inhibitor. CuBr and CuCl were purified according to the literature procedures.[45] $CuBr_2$, $CuCl_2$, ligands 2,2′-bipyridine (bpy)[14] and *N*,*N*,*N*′,*N*″,*N*″-pentamethyldiethylenetriamine (PMDETA),[46,47] and an initiator ethyl 2-bromoisobutyrate (EBiB)[48] (all from Aldrich) were used as received. All other reagents and solvents were purchased from Aldrich and used as received without further purification.

Synthesis of Trimethylsilyloxyethyl Acrylate (HEATMS). HEATMS was prepared by a modified literature procedure.[40] HEA (40.4 g, 348 mmol), triethylamine (52.7 g, 522 mmol), and dichloromethane (500.0 mL) were added to a 1000 mL round-bottom flask and cooled down to 0 °C. Chlorotrimethylsilane (56.9 g, 522 mmol) was added dropwise, and the mixture was

Published on Web 01/14/2010

stirred at 0 °C for 1 h and then overnight at room temperature. Reaction was stopped by opening the flask and filtering the salt out. The pure protected monomer, HEATMS, was obtained after distillation (45 °C, 0.06 mmHg), and the high purity was confirmed by ^{1}H NMR: ^{1}H NMR ($CDCl_3$): δ (ppm) = 6.47 (dd, J = 1.3, 17 Hz, 1H, CH_2=CH), 6.20 (dd, J = 10, 17 Hz, 1H, CH_2=CH), 5.88 (dd, J = 1.3, 10 Hz, 1H, CH_2=CH), 4.28 (t, 2H, COOCH_2), 3.88 (t, 2H, CH_2OSi), 0.18 (s, 9H, Si(CH_3)$_3$).

Synthesis of PHEATMS. HEATMS, EBiB, PMDETA, and anisole were added to a 10 mL Schlenk flask, and the reaction mixture was degassed by three freeze−pump−thaw cycles. During the final cycle, the flask was filled with nitrogen and CuBr was quickly added to the frozen mixture. The flask was sealed, evacuated, and backfilled with nitrogen three times before it was immersed in an oil bath at 60 °C. Ratio of monomer:initiator:CuBr:ligand was used as described in Table 1 (entries A1 and A2). The polymerization was stopped after 1 h by cooling the flask to room temperature and exposing the reaction mixture to air. THF was added to the reaction mixture, and the resulting polymer solution was purified by passing through a neutral alumina column.

Synthesis of Poly(2-bromoisobutyryloxyethyl acrylate) (PBiBEA). PHEATMS (6.00 g, assuming 31.9 mmol of TMS groups) was placed in a 100 mL round-bottom flask, and KF (2.26 g, 38.3 mmol) and 2,6-di-*tert*-butylphenol (0.0657 g, 0.319 mmol) were added. The flask was sealed and flushed with N_2, and dry THF (40 mL) was added. A 1.0 M solution of tetrabutylammonium fluoride in THF (0.0319 mL) was added to the flask, followed by the dropwise addition of 2-bromoisobutyl bromide (8.82 g, 38.3 mmol). The reaction mixture was stirred overnight at room temperature, and the excess of acid bromide was quenched by adding 1.0 mL of water and 1.0 mL of TEA. Solid products were separated by centrifugation. Polymer was dried overnight and purified by dialysis against THF for 48 h (1000 g/mol average pore size).

Scheme 1. Schematic Representation of the Brush and Star Architectures

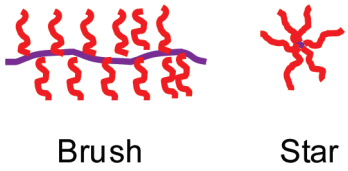

Synthesis of PBiBEA-*g*-PBA (Entries B1−B5 in Table 1). The general procedure for the preparation of the PBiBEA-*g*-PBA macroinitiator was as follows: PBiBEA, *n*-BA, PMDETA, and anisole were added to a Schlenk flask, and the reaction mixture was degassed by three freeze−pump−thaw cycles. During the final cycle, the flask was filled with nitrogen, and CuBr was quickly added to the frozen mixture. The flask was sealed, evacuated, and backfilled with nitrogen five times before it was immersed in an oil bath at 70 °C. Ratio of monomer: initiator:CuBr:$CuBr_2$: ligand was used as described in Table 1 (entries B1−B5). The resulting polymer solution was purified by passing through a column of neutral alumina. Solvent and the remaining monomer were removed under high vacuum (0.06 mmHg). The resulting product was dried at room temperature for 12 h.

Synthesis of PBiBEA-*g*-(PBA-*b*-PMMA). The general procedure for the chain extension of the PBiBEA-*g*-PBA macroinitiator was as follows: a round-bottom flask containing MMA, PBiBEA-*g*-PBA macroinitiator, $CuCl_2$, 2,2′-bipyridine, and DMF was degassed by three freeze−pump−thaw cycles. Then, CuCl was added to the frozen reaction solution under nitrogen flow. The flask was closed, evacuated, backfilled with nitrogen, and immersed in an oil bath thermostated at 50 °C. Ratio of monomer:initiator:CuCl:$CuCl_2$: ligand was used as described in Table 2 (entries C1−C10). After the polymerization was stopped, THF was added, and the polymer solution was purified by passing through a neutral alumina column. The final polymer was precipitated twice from THF to methanol.

Analysis. The molecular weight distributions and the apparent molecular weight of the polymers were determined by a GPC system, consisted of a Waters 510 HPLC pump, three Waters

Table 1. Experimental Conditions for ATRP of HEA and *n*-BA Grafted from PBiBEA and Characterization of the Prepared Polymers

entry	M	I	CuBr	$CuBr_2$	L[a]	anisole (vol %)	time (h)	conv[f] (%)	$M_{n,theor}$	$M_{n,exp}$[f]	M_w/M_n[g]	DP[f]
A1	20[b]	1[b]	0.2		0.2	10	1	92	3 650	3 960	1.24	20[g]
A2	10[b]	1[b]	0.1		0.1	10	1	90	1 890	2 080	1.21	10[g]
B1	300[c]	1[d]	0.475	0.025	0.5	6	7	38	148 000	147 000	1.13	115[h]
B2	700[c]	1[d]	0.475	0.025	0.5	6	26	34	307 000	308 000	1.14	240[h]
B3	300[c]	1[e]	0.475	0.025	0.5	6	5.5	38	296 000	294 000	1.15	115[h]
B4	700[c]	1[e]	0.475	0.025	0.5	6	21	33	596 000	590 000	1.15	230[h]
B5	2100[c]	1[e]	1.5		1.5	6	48	32	1 726 000	1 920 000	1.21	750[h]

[a] L Stands for PMDETA. [b] HEA as a monomer and EBiB as an initiator were used. [c] *n*-BA as a monomer was used. [d] PBiBEA macroinitiator, prepared from A2, with DP = 10 and M_w/M_n = 1.21. [e] PBiBEA macroinitiator, prepared from A1, with DP = 20 and M_w/M_n = 1.24. [f] Based on ^{1}H NMR spectra. [g] Based on GPC using PS standards. [h] An average DP of one PBA arm.

Table 2. Experimental Conditions for ATRP of MMA during Arms Extension of PBiBEA-*g*-PBA Starlike Copolymers and Characterization of the Prepared Copolymers[a]

entry	label	M	I	CuCl	$CuCl_2$	L	DMF (vol %)	T (°C)	time (h)	conv[g] (%)	$M_{n,theor}$[g]	M_w/M_n[h]
C1	10B115-M29	140	1[b]	1.5	0.2	3.4	49	50	6.5	21	175 000	1.20
C2	10B115-M51	140	1[b]	1.5	0.2	3.4	49	50	9.5	37	197 000	1.25
C3	10B240-M54	300	1[c]	1.5	0.2	3.4	49	50	20	20	361 000	1.20
C4	10B240-M117	300	1[c]	1.5	0.2	3.4	49	50	32.5	40	423 000	1.36
C5	20B115-M38	140	1[d]	1.8	0.15	3.9	52	50	5	24	370 000	1.28
C6	20B115-M60	140	1[d]	1.8	0.15	3.9	52	50	7	41	412 000	1.36
C7	20B230-M59	220	1[e]	1.8	0.15	3.9	52	60	6	25	706 000	1.25
C8	20B230-M107	220	1[e]	1.8	0.15	3.9	52	60	10.5	41	804 000	1.42
C9	20B750-M180	1200	1[f]	2.0	0.2	4.4	56	60	6	16	2 280 000	NA
C10	20B750-M300	1200	1[f]	2.0	0.2	4.4	56	60	10	27	2 520 000	NA

[a] M, I, and L stand for methyl methacrylate, PBiBEA-*g*-PBA macroinitiator, and bpy, respectively. [b] PBiBEA-*g*-PBA macroinitiator, prepared in entry B1, with M_n = 147 000 g/mol and M_w/M_n = 1.15. [c] PBiBEA-*g*-PBA macroinitiator, prepared in entry B2, with M_n = 308 000 g/mol and M_w/M_n = 1.15. [d] PBiBEA-*g*-PBA macroinitiator, prepared in entry B3, with M_n = 294 000 g/mol and M_w/M_n = 1.14. [e] PBiBEA-*g*-PBA macroinitiator, prepared in entry B4, with M_n = 590 000 g/mol and M_w/M_n = 1.13. [f] PBiBEA-*g*-PBA macroinitiator, prepared in entry B5, with M_n = 1 920 000 g/mol and M_w/M_n = 1.21. [g] Based on ^{1}H NMR spectra. [h] Based on GPC using PS standards.

UltraStyragel columns (guard, 10^5, 10^3, and 100 Å), and a Waters 410 differential refractive index detector, with a THF flow rate of 1.0 mL/min. Polystyrene (PS) was used as a calibration standard employing WinGPC software from Polymer Standards Service. Toluene was used as the internal standard to correct for any fluctuation in THF flow rate. Monomer conversions and molecular weights of the copolymers were determined by ^{1}H NMR on a 300 MHz Bruker NMR spectrometer using deuterated chloroform as a solvent.

Tapping Mode Atomic Force Microscopy (TMAFM). For an observation of single star macromolecules, solutions of macromolecules in chloroform (ca. 0.1 mg/mL) were spin-cast on freshly cleaved mica surfaces. For a phase-separated film morphology investigation, the block copolymers were dissolved in toluene (1 mg/mL) and were deposited by drop-casting onto silicon wafer surface (1 cm × 1 cm) cleaned by rinsing with acetone and isopropanol followed by oxygen plasma treatment. The samples were dried under house vacuum at room temperature overnight. Tapping mode AFM experiments were carried out using a Multimode Nanoscope V system (Veeco Instruments). The measurements were performed in air using commercial Si cantilevers with a nominal spring constant and resonance frequency of 5 N/m and 130 kHz or 40 N/m and 330 kHz, respectively. The height and phase images were acquired simultaneously at a set-point ratio $A/A_0 = 0.8-0.95$, where A and A_0 refer respectively to the "tapping" and "free" cantilever amplitude.

Power Spectral Analysis of TMAFM Images. Phase AFM images showing enough contrast periodicities were analyzed by a 2-D Fourier transform (FT). Subsequently, the 2-D FT maps were azimuthally averaged to produce magnitude plots analogous to the scattering patterns. After recalculating the spatial frequency scale to scattering vector units (q, $2\pi/d$), the domain spacing (d) was calculated from the q value that showed the peak maximum of the power spectrum.

Small-Angle X-ray Scattering Analysis (SAXS). SAXS measurements were conducted using a rotating anode (Rigaku RA-Micro 7) X-ray beam with a pinhole collimation and a two-dimensional detector (Bruker Highstar) with 1024 × 1024 pixels. A double graphite monochromator for the Cu Kα radiation (λ = 0.154 nm) was used. The beam diameter was about 0.8 mm, and the sample-to-detector distance was 1.8 m. The recorded scattered intensity distributions were integrated over the azimuthal angle and are presented as functions of the scattering vector ($s = 2\sin(\theta)/\lambda$, where 2θ is the scattering angle).

Dynamic Mechanical Analysis (DMA). DMA was performed on a Rheometrics RMS 800 mechanical spectrometer. Shear deformation was applied under conditions of controlled deformation amplitude, which was kept in the range of the linear viscoelastic response of studied samples. Plate−plate geometry was used with plate diameters of 6 mm. Experiments have been performed under a dry nitrogen atmosphere. Results are presented as temperature dependencies of the storage (G') and loss (G'') shear moduli measured at a constant deformation frequency of 10 rad/s. The results were obtained with a 2 °C/min heating rate.

Tensile Tests. Tensile tests were performed using a mechanical testing machine Instron 6000. Samples with thickness in the order of 0.2−0.5 mm were drawn with the rate of 5 mm/min at room temperature. Dependencies of stress vs draw ratio were recorded. Elastic modulus, elongation at break, and stress at break were determined by averaging of 3−5 independent drawing experiments performed at the same conditions.

Results and Discussion

Synthesis. The synthetic strategy for preparation of star block copolymers is illustrated in Scheme 2. ATRP was used for both the preparation of the multifunctional macroinitiator and the growth of the arms.

PBiBEA macroinitiators were prepared in three steps. In the first step, an alcohol group in HEA was protected with TMS group to form HEATMS. HEATMS was then polymerized by ATRP using EBiB initiator, PMDETA/CuBr catalyst system, and anisole as a solvent. Two different initial monomer-to-initiator ratios were used in order to prepare oligomers with different molecular weights as precursors for starlike polymers with different numbers of arms. In both cases, oligomerization was stopped once the monomer conversion reached around 90% (followed by ^{1}H NMR). Obtained oligomers were characterized by GPC (Table 1) and ^{1}H NMR (Table 1 and Figure S1). The degree of polymerization of the oligomers was calculated from ^{1}H NMR, based on the ratio of signals from PHEATMS to signals from initiator (Figure S1), and was equal to 10 and 20.

In the next step, PHEATMS oligomers were esterified with 2-bromoisobutyryl bromide in the presence of KF and 2,6-di-*tert*-butylphenol[49] (added as an inhibitor to avoid possible cross-linking) to give the multibrominated ATRP macroinitiator PBiBEA. Excess of 2-bromoisobutyric acid was removed by dialysis in THF. In a ^{1}H NMR spectrum, the signal at 0.12 ppm from methyl groups of TMS disappeared and was replaced with signal at 1.95 ppm from methyl groups of 2-bromoisobutyryl units (Figure S2). The functionalization yield, calculated from the ratio of CH_2CH_2 groups of PBiBEA to methyl groups of 2-bromoisobutyryl units, was >95% for both oligomers. Apparent molecular weights and molecular weight distributions of the oligomers determined by GPC in THF before and after functionalization were very similar.

PBA arms were grown from the PBiBEA macroinitiators using PMDETA/CuBr catalyst system in anisole as a solvent. Reaction temperature was 70 °C for all the PBA polymerizations. Three different monomer-to-initiator ratios, 300, 700, and 2100, were used for the preparation of stars with various arms length. Polymerizations were stopped at relatively low monomer conversion, between 30% and 40%, in order to minimize the star−star coupling reactions and the loss of end groups from the growing PBA chains. All polymers had narrow molecular weight distribution, as reported in Table 1. The degree of polymerization of the PBA arms was calculated from monomer conversion determined by ^{1}H NMR, assuming quantitative initiation. This is a justified assumption, since the initiation efficiency reaches 90% under similar conditions, even at lower monomer conversion and for the more congested molecular brush.[50,51]

As the ATRP equilibrium constants for MMA are much higher than that for *n*-BA, the extension of arms of PBiBEA-*g*-PBA involved the halogen exchange strategy to provide for higher, or at least comparable, rate of cross-propagation, in comparison with rate of propagation.[16,52] This approach was previously used for the successful synthesis of PBA−PMMA block copolymers.[53,54] Experimental conditions for preparation of all studied copolymers are listed in Table 2. An evolution of GPC traces with conversion for extension from PBiBEA-*g*-PBA polymers with MMA segments is shown in Figure 1. A progressive shift of the molecular weight was observed for all samples. Although polymerizations were stopped at low conversions, up to 40%, a tail toward the higher molecular weights was observed in most of the polymers due to intermolecular radical coupling between the growing arms of the stars. The fraction of coupled stars increased with arm length (increased with a monomer conversion) as well as number of arms.

During extension of PBiBEA-*g*-PBA stars with the DP of PBA arms equal to 750 (Table 2, entries C9 and C10), intermolecular coupling reactions between PBiBEA-*g*-(PBA-*b*-PMMA) stars formed gels that could not be filtered through a

Scheme 2. Synthesis of Star Copolymers

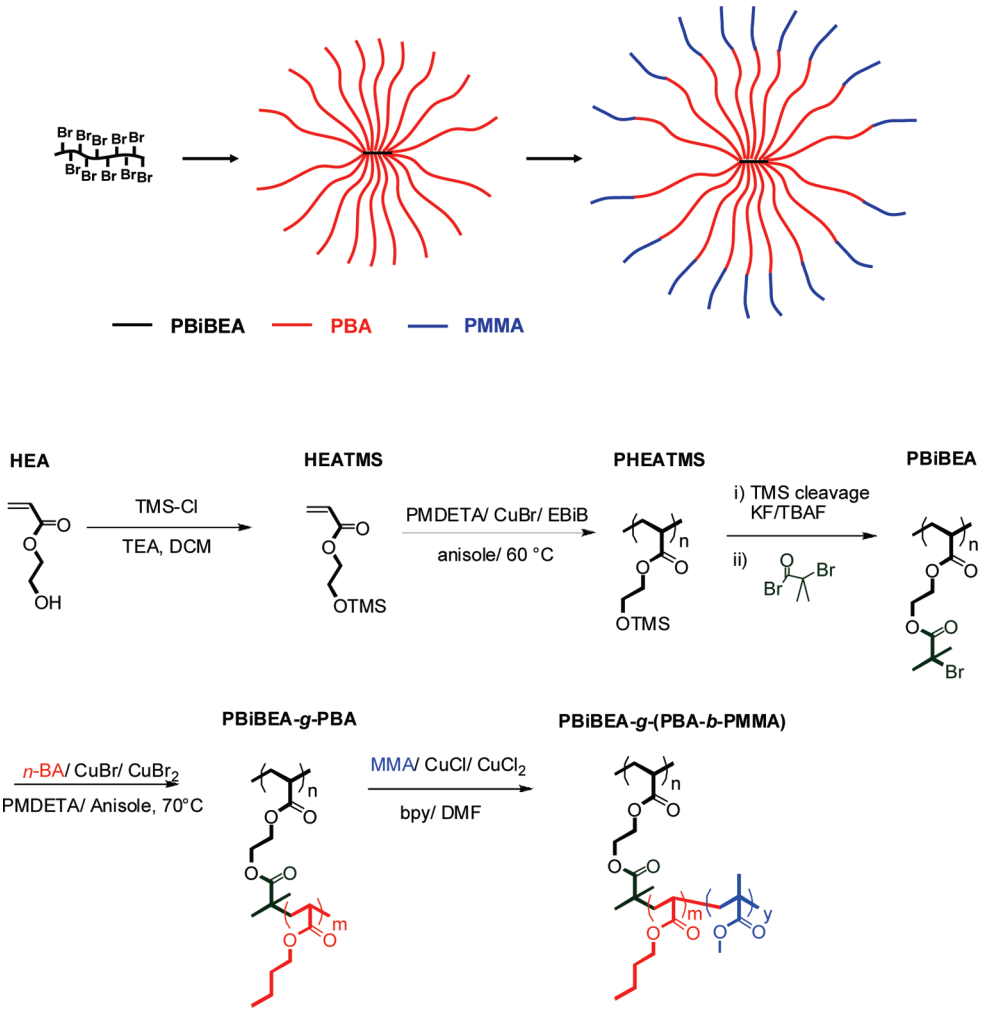

0.2 μm filter. The degree of polymerization of the PMMA blocks was calculated from ^{1}H NMR spectra based on the ratio of signals from PBA to PMMA (Figure S4, signal i to signal c). The compositions of the prepared starlike block copolymers determined by NMR are listed in Table 3.

AFM Visualization of Stars and Morphology of the PBiBEA-*g*-(PBA-*b*-PMMA) Starlike Block Copolymers. In order to observe the individual star macromolecules, dilute solutions (0.1−0.001 mg/mL) of PBiBEA$_{10}$-*g*-PBA$_{240}$ as well as 10B240-M54 and 10B240-M117 star polymers were cast on a mica surface. In Figure 2 (AFM pictures a and e), single PBiBEA$_{10}$-*g*-PBA$_{240}$ stars are seen. The number of arms in each molecule was around 10, showing a good agreement with the anticipated values. The end-to-end distance of PBiBEA$_{10}$-*g*-PBA$_{240}$ measured using the AFM images is around 60 nm. For comparison, the maximal end-to-end distance of PBiBEA$_{10}$-*g*-PBA$_{240}$ for fully extended conformation should be around 120 nm. Interestingly, the end-to-end distances of the stars after arms extension with PMMA block did not increase. The end-to-end distances of 10B240-M54 and 10B240-M117 from the AFM images are around 45 and 60 nm, respectively. While the PBA blocks of low T_g (−50 °C) relaxed to random coils on the mica surface, the PMMA blocks (T_g = 130 °C) are plausibly placed on the top of PBA chains, forming objects with a more spherelike shape. This conclusion is supported also by the AFM images obtained by casting the solutions of 10B240-M117 at 10 times higher concentration (Figure 2, pictures d and h) than that used for a single molecule imaging. In this case, even though the concentration is not sufficient for a film formation, a strong phase separation is observed, where PBA blocks are still stretched on the surface, but PMMA blocks aggregate and ascend from the surface. A similar behavior was reported earlier for brush macromolecules with block copolymer architecture containing a PBA core and a polystyrene shell.[55]

Incompatibility between PBA and PMMA blocks should cause nanoscale phase separation in bulk materials. Thin films were prepared by drop-casting of more concentrated (1 mg/mL) polymer solutions in toluene onto silicon wafer substrates and studied by AFM (Figure 3). AFM images showed a cylindrical morphology for all prepared starlike block copolymers except the 10B115-M29. SAXS analysis of thick films of the starlike block copolymers (Figure S5) confirmed that the majority of the samples reveal a microphase-separated morphology of cylindrical PMMA domains hexagonally arranged in the PBA matrix (three peaks at relative positions s, $3^{1/2}s$, $7^{1/2}s$). Again, the samples with shortest arm length and lowest PMMA content, 10B115-M29 and 20B115-M38, did not reveal a clear structure. They exhibited a short-range ordering only, as indicated from the single broad peak observed in the SAXS spectra. The different compositions of the 10-arm and 20-arm PBA−PMMA copolymers affected the d-spacing in the microphase-separated structures. Table 3 shows the values of the d-spacing obtained from AFM and SAXS data of the

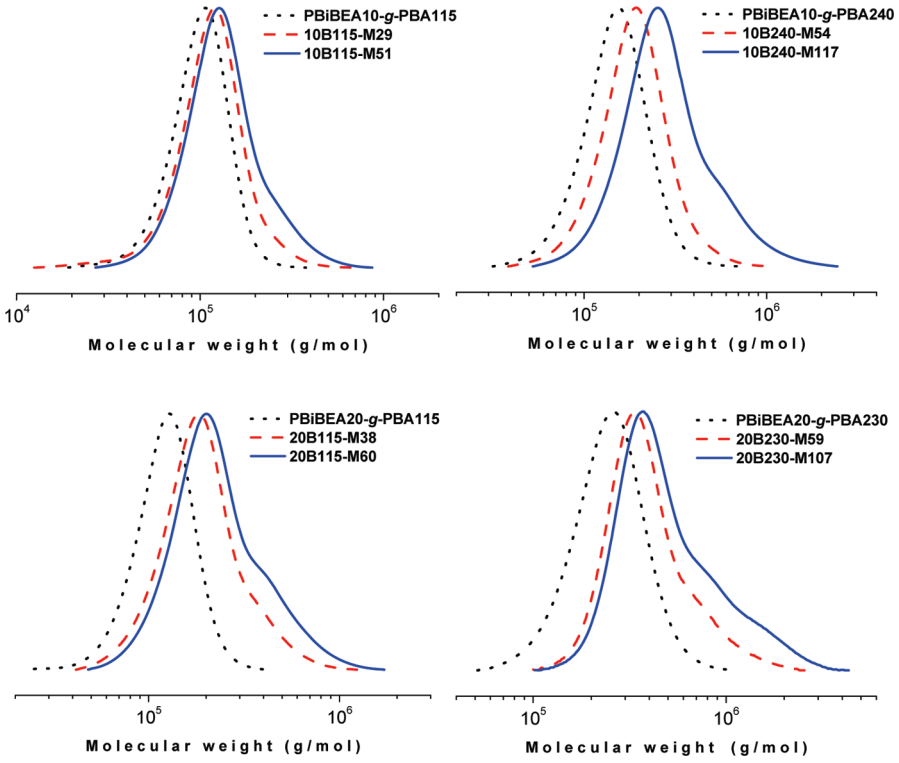

Figure 1. GPC traces of PBiBEA-*g*-(PBA-*b*-PMMA) starlike block copolymers prepared by arms extension from PBiBEA-*g*-PBA starlike macroinitiators.

Table 3. Compositions of the Prepared PBiBEA-*g*-(PBA-*b*-PMMA) Starlike Block Copolymers and Their Phase Separation Spacing Values in Thin Films

					spacing (nm)	
entry	label	triblock composition	PMMA (mol %)[a]	PMMA (wt %)[a]	AFM	SAXS
C1	10B115-M29	$PBiBEA_{10}$-(PBA_{115}-$PMMA_{29}$)$_{10}$	20.1	16.4		22
C2	10B115-M51	$PBiBEA_{10}$-(PBA_{115}-$PMMA_{51}$)$_{10}$	30.7	25.7	27	24
C3	10B240-M54	$PBiBEA_{10}$-(PBA_{240}-$PMMA_{54}$)$_{10}$	18.4	14.9	32	30
C4	10B240-M117	$PBiBEA_{10}$-(PBA_{240}-$PMMA_{117}$)$_{10}$	32.8	27.6	39	38
C5	20B115-M38	$PBiBEA_{20}$-(PBA_{115}-$PMMA_{38}$)$_{20}$	24.8	20.5	24	23
C6	20B115-M60	$PBiBEA_{20}$-(PBA_{115}-$PMMA_{60}$)$_{20}$	34.3	28.9	26	24
C7	20B230-M59	$PBiBEA_{20}$-(PBA_{230}-$PMMA_{59}$)$_{20}$	20.4	16.7	39	33
C8	20B230-M107	$PBiBEA_{20}$-(PBA_{230}-$PMMA_{107}$)$_{20}$	31.8	26.6	37	35
C9	20B750-M180	$PBiBEA_{20}$-(PBA_{750}-$PMMA_{180}$)$_{20}$	19.4	15.8	63	63
C10	20B750-M300	$PBiBEA_{20}$-(PBA_{750}-$PMMA_{300}$)$_{20}$	28.6	23.8	59	73

[a] Based on ^{1}H NMR spectra.

measured PBA−PMMA star block copolymers. As can be seen in Table 3, the increase of PMMA block length leads to an increase in the *d*-spacing for copolymers with the same length of the PBA segment. The number of arms has a negligible influence on *d*-spacing.

In order to examine the effect of thermal treatment on the copolymer films morphology, the SAXS experiments were repeated after annealing the PBA−PMMA copolymer samples at 150 °C. The experiment showed that there was no loss of phase separation after annealing for 60 min, and the annealed films exhibited even better ordering than the untreated samples, displaying at least three scattering peaks in each of the SAXS spectra. The ratios of the relative peak positions was s, $3^{1/2}s$, $7^{1/2}s$, consistent with a hexagonal lattice. An example the SAXS spectra of thick film of 20B115-M60 measured before and after annealing is presented in Figure 4.

Thermomechanical Properties of the PBiBEA-*g*-(PBA-*b*-PMMA) Starlike Block Copolymers. Dynamic mechanical properties of the multiarm stars PBA−PMMA block copolymers were characterized through the temperature dependencies of the real (G') and the imaginary (G'') parts of the complex shear modulus. Typical results obtained for two 20-arm star block copolymers with different arm compositions (20B230-M59 and 20B230-M107) are shown in Figure 5a. The existence of two distinct glass transitions corresponding to the PBA ($T_g \sim -50$ °C) and PMMA ($T_g \sim 130$ °C) segments is clearly observed for 20B230-M107 but less pronounced for 20B230-M59. This constitutes a further evidence for the microphase-separated morphology of the star block copolymers. With respect to the mechanical properties, both samples were glassy below the glass transition temperature of PBA, with storage modulus $G' \sim 1$ GPa. Above this glass transition, the copolymers became elastic and showed a rubbery plateau ($G' < 1$ MPa) extending up to the softening temperature of PMMA (~130 °C). In this elastic state, the PMMA blocks form glassy domains that comprise PMMA segments from different star copolymer molecules, connecting in this way the flexible PBA blocks. This is a typical situation for a thermoplastic elastomer,

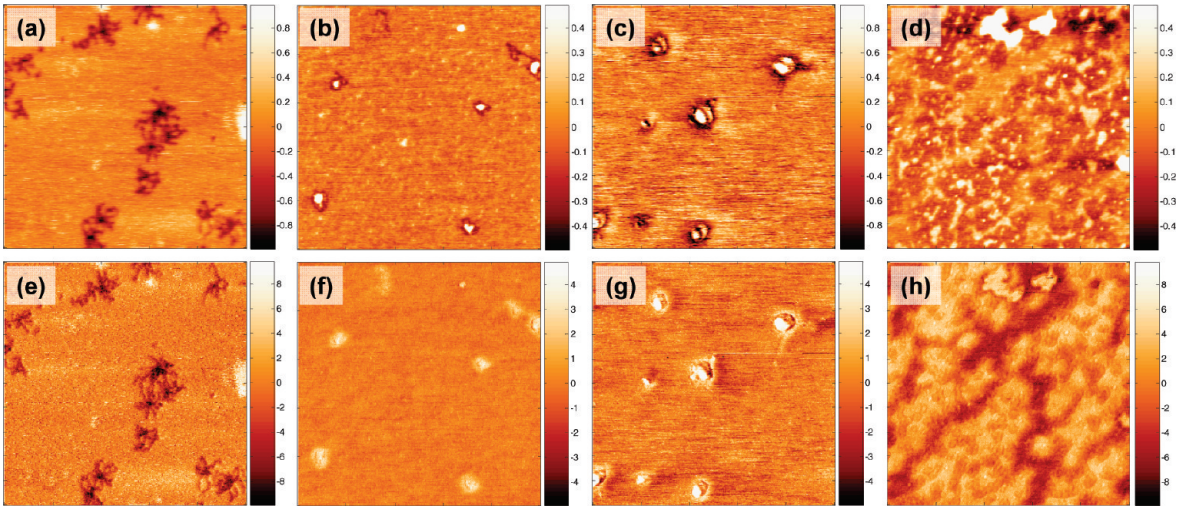

Figure 2. (a−d) Height and (e−h) phase mode AFM images of starlike polymers: (a, e) $PBiBEA_{10}$-*g*-PBA_{240} prepared by drop-casting of a 0.001 mg/mL solution; (b, f) 10B240-M54 prepared by spin-casting of a 0.01 mg/mL solution; (c, g) 10B240-M117 prepared by spin-casting of a 0.01 mg/mL solution; and (d, h) 10B240-M117 prepared by spin-casting of a 0.1 mg/mL solution. Image size = 0.6 × 0.6 μm^2. Negative height contrast in the height mode is due to the artifact originated from the stickiness of PBA chains. Units of scale bars in height images "nm" and in phase images "degree (°)".

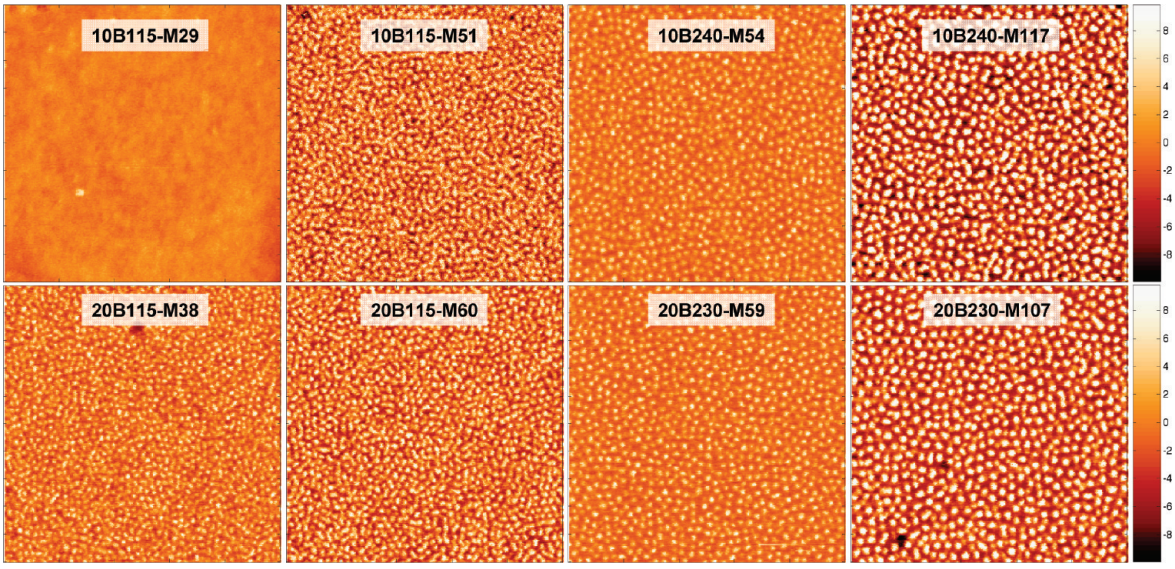

Figure 3. Phase mode AFM images of film samples. Image size = 1 × 1 μm^2. Unit of scale bars in "degree (°)".

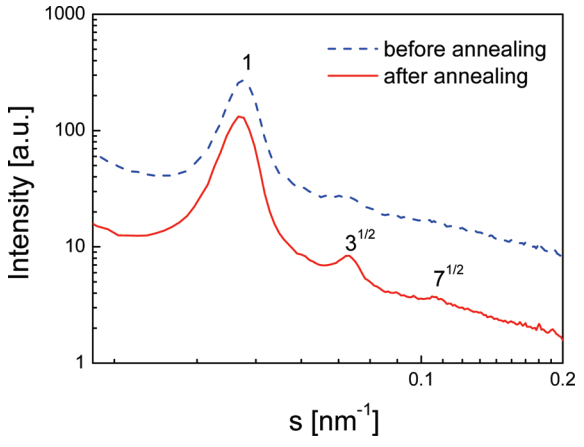

Figure 4. SAXS spectra of 20B115-M60 before and after annealing at 150 °C for 60 min.

in which the hard phase elements (i.e., the glassy PMMA microdomains) act as physical cross-links for the soft PBA matrix. The degree of elasticity depends on the composition; i.e., the sample with lower PMMA content has a smaller G' value in the rubbery plateau region. The thermomechanical properties at higher temperatures also depend on the copolymer composition. While both materials retained the phase-separated morphology and low modulus rubbery behavior well above the PMMA glass transition, the copolymer 20B230-M59, with only a 16.7% PMMA content, eventually starts flowing at a temperature around 250 °C. On other hand, the copolymer 20B230-M107 did not flow in the entire temperature range studied, i.e., up to 300 °C.

Figure 5b illustrates the effect of the overall molecular weight on the mechanical properties of the star copolymers by comparing the DMA spectra of 20B115-M38, 20B230-M59, and 20B750-M180, three materials that have similar compositions but significantly different molecular weights.

As can be seen, the high molecular weight copolymers (20B230-M59 and 20B750-M180) retain the phase-separated morphology and low modulus rubbery behavior well above the PMMA glass transition. In contrast, the low molecular weight copolymer 20B115-M38 starts flowing at 200 °C. In spite of their very different molecular weights, all three copolymers have very similar values of the storage modulus G' in the rubbery plateau region between the glass transition temperatures of the two components. This indicates that the copolymer composition rather than the overall molecular weight is the main factor that determines the elastic properties of these thermoplastic elastomer materials.

Another parameter that could influence the thermomechanical properties of the starlike copolymers is the number of arms. Figure 5c compares the DMA spectra of a 10- and 20-arm star copolymers with similar block lengths and compositions: 10B240-M117 and 20B230-M107. The two materials show practically identical spectra, which indicates that the number of arms have little influence on their mechanical properties. This is not surprising since both materials should have a sufficiently large number of arms, i.e., 10 and 20, respectively. Indeed, earlier studies of polystyrene-*b*-polyisobutylene[35] and polystyrene-*b*-polydiene[56] starlike block copolymers showed that the tensile properties of these materials reach a plateau in the $N_{arm} = 5-10$ range. Evidently, the presence of such a plateau explains the similar mechanical properties of the 10- and 20-arm PBA−PMMA star block copolymers. Comparable behavior could be expected for the block copolymer brushes having higher number of arms; however, stress around the congested backbone could reduce tensile properties.

The tensile properties of every star block copolymers listed in Table 4 were studied. Typical examples of the measured stress−strain dependencies are shown in Figure 6. The composition has a major effect on the tensile properties of the PBA−PMMA star copolymers. Both the initial modulus (E) and the tensile strength (σ break) increase strongly with PMMA content. The tensile strength increased linearly with PMMA content and did not depend on the total length of the arms or total molecular weight of the copolymers (see Figure S6). The draw ratio at break increased with the length of PBA segment and decreased with increasing PMMA content.

It was previously reported that thermoplastic elastomers based on star block copolymers[33−39] may exhibit superior properties in comparison with the linear ABA triblock type TPEs. It was also shown[34,49] that the tensile properties of the star block copolymers improved with the number of arms until reaching saturation at the $N_{arm} = 5-10$. In an attempt to explore these effects for PBA−PMMA-based materials, we compared the newly synthesized 10- and 20-arm 10B115-M51 and 20B115-M60 copolymers with the 3-arm star copolymer 3B164-M76 that we have recently studied[33] and to a linear PMMA−PBA−PMMA block copolymer prepared using ATRP by another group.[57] As shown in Table 4, all four materials have similar overall composition and also similar arm molecular weight. The stress−strain dependencies for the three star-shaped block copolymers are shown in Figure 6b, and the tensile properties of all four materials are summarized in Table 4. There is a clear increase in ultimate tensile strength and the elastic modulus with the increase in number of arms. Particularly, the ultimate tensile strength of

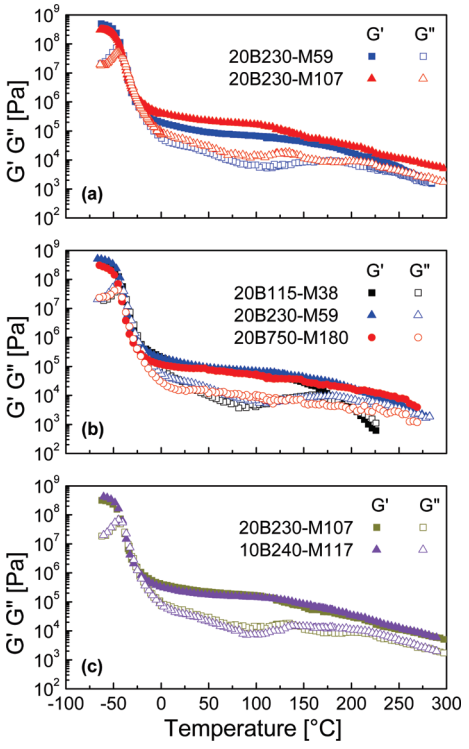

Figure 5. DMA spectra of the star PBA−PMMA block copolymer (a) 20B230-M59, 20B230-M107, (b) 20B115-M38, 20B230-M59, 20B750-M180, and (c) 20B230-M107, 10B240-M117.

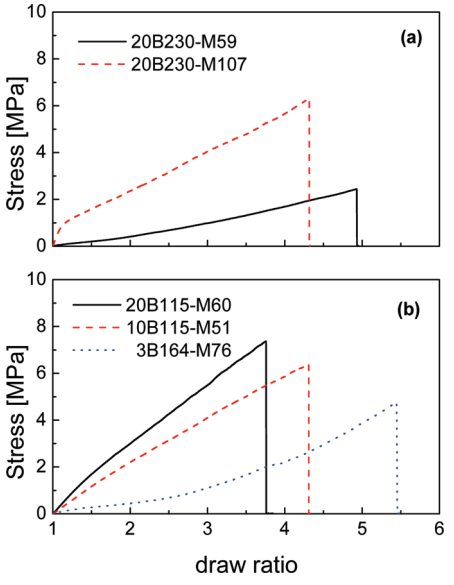

Figure 6. Tensile properties of copolymers (a) 20B230-M59, 20B230-M107 and (b) 20B115-M60, 10B115-M51, 3B164-M76.

Table 4. Ultimate Tensile Strength and Maximum Elongation at Break of PBA−PMMA Block Copolymers with Similar Composition but Varying Numbers of Arms

sample	M_n (g/mol)	PDI	PMMA content (wt %)	ultimate tensile strength σ (MPa)	maximum elongation at break λ (%)
linear ABA type copolymer[57]	69 000	1.15	26	4.2	520
3-arm star B164-M76 block copolymer[33]	85 800	1.19	26	4.8	545
10-arm B115-M51 copolymer	197 000	1.25	25.7	6.4	430
20-arm B115-M60 copolymer	412 000	1.36	28.9	7.4	375

the 10-arm 10B115-M51 is much higher than that of the linear and the 3-arm copolymer. As discussed by Shim and Kennedy,[34] this behavior could originate in several effects. First, in addition to the PMMA glassy domains that act as physical cross-linkers for the softer PBA matrix in the case of star copolymers, small permanent cross-linking sites, i.e., the cores of star blocks, are also dispersed in the rubbery matrix, helping to distribute the applied stress more evenly to the hard PMMA domains. Second, the multiarm stars exhibit higher degree of hard-domain interconnectivity between the copolymer molecules. The improvement of tensile strength is less significant when comparing the 10-arm vs the 20-arm samples, which suggests again a plateau or saturation point in the enhancement of the tensile properties with respect to number of arms. This is consistent with earlier studies of polystyrene-*b*-polyisobutylene[35] and polystyrene-*b*-polydiene[56] starlike copolymers and is related to the fact that the contribution of the above-described effects saturates with increasing the number of arms. Furthermore, increasing the number of arms affects the chain conformation and decreases their mobility which may influence the phase separation.

Conclusions

In summary, PBiBEA macroinitiators for starlike copolymers with degrees of polymerizations 10 and 20 were prepared by ATRP of HEATMS and the subsequent esterification. These macroinitiators were used for preparation of series of 10- and 20-arm starlike PBA which were extended with outer hard PMMA block using ATRP. Halogen exchange strategy was applied during the ATRP of PMMA to provide at least equal rate of cross-propagation compared to rate of propagation.[52] Partial star coupling during PBA arms extension with PMMA blocks was observed, and the coupling increased with number of arms and arm length. The morphology of solution-cast films of the star PBA−PMMA block copolymers was studied by AFM and SAXS. Both techniques revealed a phase-separated morphology of cylindrical PMMA domains hexagonally arranged in the PBA matrix. The mechanical and thermal properties of the star block copolymers have been thoroughly characterized. These materials possess typical elastomeric behavior in a broad range of service temperatures up to at least 250 °C. The ultimate tensile strength and the elastic modulus of the 10- and 20-arm star PBA−PMMA copolymers are significantly higher than those of their 3-arm or linear ABA type counterparts with similar composition, indicating a strong effect of the number of arms on the tensile properties. This new synthetic approach can be used for the preparation of star polymers from other acrylates, methacrylates, and styrene.

Acknowledgment. The authors thank Andreas Hanewald for the technical assistance. The financial support from National Science Foundation (DMR 05-49353 and CBET 06-09087) is greatly appreciated.

Supporting Information Available: Dependence of ultimate tensile strength on PMMA content and NMR and SAXS traces. This material is available free of charge via the Internet at http://pubs.acs.org.

References and Notes

(1) Zhang, M.; Mueller, A. H. E. *J. Polym. Sci., Part A: Polym. Chem.* **2005**, *43*, 3461–3481.
(2) Sheiko, S. S.; Sumerlin, B. S.; Matyjaszewski, K. *Prog. Polym. Sci.* **2008**, *33*, 759–785.
(3) Gao, H.; Matyjaszewski, K. *Prog. Polym. Sci.* **2009**, *34*, 317–350; Oh, J. K.; Drumright, R.; Siegwart, D. J.; Matyjaszewski, K. *Prog. Polym. Sci.* **2008**, *33*, 448–477.
(4) Hadjichristidis, N.; Iatrou, H.; Pitsikalis, M.; Mays, J. *Prog. Polym. Sci.* **2006**, *31*, 1068–1132.
(5) Gao, C.; Yan, D. *Prog. Polym. Sci.* **2004**, *29*, 183–275.
(6) Gaynor, S. G.; Matyjaszewski, K. *Macromolecules* **1997**, *30*, 4241–4243.
(7) Szwarc, M. *Science* **1970**, *170*, 23–31.
(8) Bielawski, C. W.; Grubbs, R. H. *Prog. Polym. Sci.* **2007**, *32*, 1–29.
(9) Braunecker, W. A.; Matyjaszewski, K. *Prog. Polym. Sci.* **2007**, *32*, 93–146.
(10) Debuigne, A.; Poli, R.; Jerome, C.; Jerome, R.; Detrembleur, C. *Prog. Polym. Sci.* **2009**, *34*, 211–239.
(11) Hawker, C. J.; Bosman, A. W.; Harth, E. *Chem. Rev.* **2001**, *101*, 3661.
(12) Moad, G.; Rizzardo, E.; Thang, S. H. *Aust. J. Chem.* **2005**, *58*, 379–410.
(13) Chiefari, J.; Chong, Y. K.; Ercole, F.; Krstina, J.; Jeffery, J.; Le, T. P. T.; Mayadunne, R. T. A.; Meijs, G. F.; Moad, C. L.; Moad, G.; Rizzardo, E.; Thang, S. H. *Macromolecules* **1998**, *31*, 5559–5562.
(14) Wang, J. S.; Matyjaszewski, K. *J. Am. Chem. Soc.* **1995**, *117*, 5614–5615.
(15) Tsarevsky, N. V.; Matyjaszewski, K. *Chem. Rev.* **2007**, *107*, 2270–2299.
(16) Matyjaszewski, K.; Xia, J. H. *Chem. Rev.* **2001**, *101*, 2921–2990.
(17) Matyjaszewski, K.; Tsarevsky, N. V. *Nat. Chem.* **2009**, *1*, 276–288.
(18) Kamigaito, M.; Ando, T.; Sawamoto, M. *Chem. Rev.* **2001**, *101*, 3689–3746.
(19) Gao, H.; Matyjaszewski, K. *Macromolecules* **2006**, *39*, 4960–4965.
(20) Matyjaszewski, K. *Polym. Int.* **2003**, *52*, 1559–1565.
(21) Zhang, X.; Xia, J.; Matyjaszewski, K. *Macromolecules* **2000**, *33*, 2340–2345.
(22) Xia, J.; Zhang, X.; Matyjaszewski, K. *Macromolecules* **1999**, *32*, 4482–4484.
(23) Radke, W.; Gerber, J.; Wittmann, G. *Polymer* **2002**, *44*, 519–525.
(24) Matyjaszewski, K.; Miller, P. J.; Pyun, J.; Kickelbick, G.; Diamanti, S. *Macromolecules* **1999**, *32*, 6526–6535.
(25) Ueda, J.; Matsuyama, M.; Kamigaito, M.; Sawamoto, M. *Macromolecules* **1998**, *31*, 557–562.
(26) Angot, S.; Murthy, K. S.; Taton, D.; Gnanou, Y. *Macromolecules* **1998**, *31*, 7218–7225.
(27) Hawker, C. J. *Angew. Chem., Int. Ed.* **1995**, *34*, 1456–1459.
(28) Danko, M.; Libiszowski, J.; Wolszczak, M.; Racko, D.; Duda, A. *Polymer* **2009**, *50*, 2209–2219.
(29) Hans, M.; Mourran, A.; Henke, A.; Keul, H.; Moeller, M. *Macromolecules* **2009**, *42*, 1031–1036.
(30) Wang, J.-S.; Greszta, D.; Matyjaszewski, K. *Polym. Mater. Sci. Eng.* **1995**, *73*, 416–417.
(31) Gao, H.; Matyjaszewski, K. *Macromolecules* **2008**, *41*, 1118–1125.
(32) Lapienis, G. *Prog. Polym. Sci.* **2009**, *34*, 852–892.
(33) Dufour, B.; Koynov, K.; Pakula, T.; Matyjaszewski, K. *Macromol. Chem. Phys.* **2008**, *209*, 1686–1693.
(34) Dufour, B.; Tang, C. B.; Koynov, K.; Zhang, Y.; Pakula, T.; Matyjaszewski, K. *Macromolecules* **2008**, *41*, 2451–2458.
(35) Shim, J. S.; Kennedy, J. P. *J. Polym. Sci., Part A: Polym. Chem.* **1999**, *37*, 815–824.
(36) Shim, J. S.; Kennedy, J. P. *J. Polym. Sci., Part A: Polym. Chem.* **2000**, *38*, 279–290.
(37) Shim, J. S.; Asthana, S.; Omura, N.; Kennedy, J. P. *J. Polym. Sci., Part A: Polym. Chem.* **1998**, *36*, 2997–3012.
(38) Storey, R. F.; Chrisholm, B. J.; Choate, K. R. *J. Polym. Sci., Part A: Polym. Chem.* **1994**, *34*, 2003–2017.
(39) Storey, R. F.; Shoemake, K. A. *J. Polym. Sci., Part A: Polym. Chem.* **1998**, *36*, 471–483.
(40) Beers, K. L.; Gaynor, S. G.; Matyjaszewski, K.; Sheiko, S. S.; Moeller, M. *Macromolecules* **1998**, *31*, 9413–9415.
(41) Neugebauer, D.; Zhang, Y.; Pakula, T.; Sheiko, S. S.; Matyjaszewski, K. *Macromolecules* **2003**, *36*, 6746–6755.
(42) Sheiko, S. S.; Prokhorova, S. A.; Beers, K. L.; Matyjaszewski, K.; Potemkin, I. I.; Khokhlov, A. R.; Moller, M. *Macromolecules* **2001**, *34*, 8354–8360.
(43) Sheiko, S. S.; Sun, F. C.; Randall, A.; Shirvanyants, D.; Rubinstein, M.; Lee, H.; Matyjaszewski, K. *Nature* **2006**, *440*, 191–194.
(44) Qin, S.; Matyjaszewski, K.; Xu, H.; Sheiko, S. S. *Macromolecules* **2003**, *36*, 605–612.
(45) Keller, R. N.; Wycoff, H. D. *Inorg. Synth.* **1946**, *2*, 1–4.
(46) Xia, J. H.; Matyjaszewski, K. *Macromolecules* **1997**, *30*, 7692–7696.
(47) Pintauer, T.; Matyjaszewski, K. *Coord. Chem. Rev.* **2005**, *249*, 1155–1184.

(48) Wang, J.-S.; Matyjaszewski, K. *Macromolecules* **1995**, *28*, 7901–7910.
(49) Park, I.; Sheiko, S. S.; Nese, A.; Matyjaszewski, K. *Macromolecules* **2009**, *42*, 1805–1807.
(50) Neugebauer, D.; Sumerlin, B. S.; Matyjaszewski, K.; Goodhart, B.; Sheiko, S. S. *Polymer* **2004**, *45*, 8173–8179.
(51) Sumerlin, B. S.; Neugebauer, D.; Matyjaszewski, K. *Macromolecules* **2005**, *38*, 702–708.
(52) Matyjaszewski, K.; Shipp, D. A.; Wang, J. L.; Grimaud, T.; Patten, T. E. *Macromolecules* **1998**, *31*, 6836–6840.
(53) Matyjaszewski, K.; Shipp, D. A.; McMurtry, G. P.; Gaynor, S. G.; Pakula, T. *J. Polym. Sci., Part A: Polym. Chem.* **2000**, *38*, 2023–2031.
(54) Shipp, D. A.; Wang, J.-L.; Matyjaszewski, K. *Macromolecules* **1998**, *31*, 8005–8008.
(55) Boerner, H. G.; Beers, K.; Matyjaszewski, K.; Sheiko, S. S.; Moeller, M. *Macromolecules* **2001**, *34*, 4375–4383.
(56) Bi, L. K.; Fetters, L. J. *Macromolecules* **1976**, *9*, 732–742.
(57) Tong, J. D.; Moineau, G.; Leclere, P.; Bredas, J. L.; Lazzaroni, R.; Jerome, R. *Macromolecules* **2000**, *33*, 470–479.